

## Research Article

# Modeling of Nanolubricant-Assisted Machining Process by using Multiple Regression Analysis

S. Srikanth <sup>1</sup>, P. N. L. Pavani <sup>2</sup> and Kumaran Palani <sup>3</sup>

<sup>1</sup>Centre for Nanotechnology, College of Engineering, Andhra University, Visakhapatnam, India

<sup>2</sup>Department of Mechanical Engineering, GMR Institute of Technology, Rajam, India

<sup>3</sup>Department of Mechanical Engineering, College of Engineering, Wolaita Sodo University, Wolaita Sodo, Ethiopia

Correspondence should be addressed to Kumaran Palani; pkumaran2003et@gmail.com

Received 11 September 2022; Revised 13 January 2023; Accepted 16 January 2023; Published 14 February 2023

Academic Editor: Mazeyar Parvinzadeh Gashti

Copyright © 2023 S. Srikanth et al. This is an open access article distributed under the Creative Commons Attribution License, which permits unrestricted use, distribution, and reproduction in any medium, provided the original work is properly cited.

Graphite, due to its hexagonally arranged crystal structure, is a preferred lubricant. The crystal structure within a planar condensed ring system indicates that the layers are stacked in a direction that is parallel to each other. Researchers have reported that the use of graphite powder as a lubricant during machining has exhibited promising results. Mixture of graphite in a carrying medium demonstrated multifunctional lubrication performance due to the separation of sliding surfaces by a liquid lubricant film and protected by solid powder. Scientific literature has pointed out that graphite powder at the nanoscale has been used in various mechanical operations exhibiting promising results. It is found that nanolevel graphite powder has been used previously by researchers in the metal-forming operations and tribological tests. This emphasizes the significance of the present work, which investigates the impact of nanoscale differences in the particle size of graphite powder has on the machining of hardened steel. With SAE 40 oil functioning as the carrying medium and nanocrystalline graphite of various size range performing as the lubricant, the current work attempts to determine the effects of solid-lubricant-assisted machining. It is observed experimentally that the machining parameters have improved with respect to the particle size of the nanopowder. The experimental results show that the cutting forces, tool temperatures, and surface roughness are found to increase as the size of the nanocrystalline graphite powder is reduced from 70–90 to 5–10 nm. Using the experimental values, regression analysis is carried out to develop nonlinear expressions between the input and output variables using SPSS statistical tool. The data are used to develop the models to predict cutting forces, tool temperatures, and surface roughness for the input parameters like size of the nanocrystalline graphite powder, depth of cut, feed rate, and cutting velocity for a considerably good range in a scientific way so that further researchers can use it. Further, the outputs obtained from the experimentation and the regression equations are compared and analysis is carried out in terms of the error percentage.

## 1. Introduction

Machining process is perceived to be a dynamic process and is influenced by a wide range of variables making the process complicated to be understood. Hence, there is a need to mathematically predict and optimization processes for the benefit of the machinists. There is a dire need of finding out eco-friendly and user-friendly alternative cutting fluids and lubricants to cater to the need of high-speed machining which generates high cutting temperatures. These temperatures not only reduce tool life but also degrades product quality. In pursuit of newer lubricants, the technological advancements in modern tribology have led to an increase

in the adoption of effective unconventional procedures such as dry cutting, cryogenic cooling, minimum quantity lubrication (MQL), and the use of solid lubricants. Recent experimental investigations have noted that boric acid and boron-containing compounds, such as MoS<sub>2</sub> and graphite, have the ability to self-lubricate and are employed in practical applications as solid lubricants. Additionally, it has been said that in humid environments, they offer higher lubricating properties.

It is found that various researchers have used graphite as lubricant and practically demonstrated that it is better than the conventional standard coolants used. This phenomenon is visible even in grinding process [1], wherein it is observed

that the overall process variables improved [2], which includes grinding forces [3], temperature [4], specific energy, and surface roughness [5] which were observed and found to be lessened as compared with grinding with a standard coolant [6, 7]. There are investigative reports which exhibited better results in terms of lowered friction coefficient [8] at the tool–chip interface during cutting of hardened steel while using  $\text{Al}_2\text{O}_3/\text{TiC}/\text{CaF}_2$  as a lubricant. With the use of graphite and molybdenum disulfide in end milling, it is revealed that there is a significant improvement in its performances in terms of cutting forces, surface quality, and specific energy [9] as compared with using only cutting fluid.

The machining characteristics of SAE 40 oil with different weight ratios of graphite and boric acid were investigated when turning EN 8 steel [9]. Cutting force, tool wear, cutting temperature, and surface finish were looked at in order to gauge the effect of solid lubricants on machining performance. Although both solid lubricants and dry machining resulted in greater machining performance than traditional cutting fluids, 20% boric acid in SAE 40 oil offered superior performance for the chosen tool–work combination and cutting conditions. There are researchers who have used simultaneously all four types of lubricating conditions during machining operations [10, 11].

There are research findings of the use of  $\text{MoS}_2$  [12–14] as a lubricant which demonstrated significant improvement in the cutting parameters and even established equations with respect to cutting parameters [15] and surface roughness [16] of the job [17, 18]. Studies have been conducted by the use of  $\text{MoS}_2$  as cutting fluid to the regular cutting fluid along with the use of  $\text{MoS}_2$ -coated ceramic tool [19]. The findings demonstrated that ceramic cutting tools with  $\text{MoS}_2$  coatings had significantly longer wear lives and experienced less flank wear. Analysis was done on the life-extension mechanisms. Self-lubricating low friction  $\text{MoS}_2/\text{Ti}$  composite coatings of  $1\text{ }\mu\text{m}$  thickness were applied on hard-coated carbide inserts using a hybrid technique to assess ceramic inserts for dry high-speed milling and turning of steel [20]. The coatings were put to the test while being subjected to dry conditions, rapid milling, and turning operations at high temperatures. The performance of the tools was found to be influenced by cutting tools' shape, grade, and parameters.

By constantly removing the heat from the machining zone, solid lubricant can efficiently manage the temperature there. To investigate the impact of solid lubricant on surface polish, experiments were conducted [21, 22]. When cutting AISI 1040 steel with uncoated cemented carbide inserts, the use of solid lubricants successfully reduced the surface roughness and chip thickness ratio compared with wet machining [23]. The use of  $\text{MoS}_2$  in machining had resulted in a 5%–30% improvement in surface finish. Similar occurrences in terms of surface roughness are seen when bearing steel is subjected to strong turning [24]. Using  $\text{MoS}_2$  results in a better surface polish. This study also revealed that the ideal rake angle for solid lubricants was higher ( $12^\circ$ ) than it was for wet machining ( $8^\circ$ ), indicating that sharper tools can be used during machining in the presence of solid lubricants to increase the machinability of AISI 1040 steel material.

Therefore, the increased machinability from the decreased friction in solid-lubricant-aided machining leads to greater material removal rates without impacting the quality of the surface produced, thereby enhancing product reliability, increasing productivity, and decreasing cost. Researchers have also observed that the use of hybrid nanolubricants [25] in base oil has affected the machining parameters. It was also observed during the use of MWCNT and  $\text{Al}_2\text{O}_3$  in SAE 50 oil [26].

It was observed that the particle size of the solid lubricants affects its tribological and machining properties [19–21, 27]. The smaller particles exhibit superior performance as compared with larger particle sizes. Graphite powder spray was used to apply graphite particles of 50, 100, 150, and  $200\text{ }\mu\text{m}$  sizes while hardened steel was being machined [21]. Keeping the cutting variables constant, the process's effectiveness was assessed in terms of cutting force, tool temperature, tool wear, and the workpiece's surface polish. Observations show that graphite with  $50\text{ }\mu\text{m}$  particle size has a more efficient lubricating effect. Similar phenomenon was observed in the turning of AISI 1040 steel [19] and in hard turning process [20]. This phenomenon is also observed in milling operations [27] where the grinding force is found to be minimum when smaller particle sizes of the solid lubricants are used. The key to this performance of graphite is its layer lattice structure and low coefficient of friction. The superiority of smaller graphite particles is because of their more adhesion tendency.

The various machining experimentations conducted with the use of solid lubricants show that they exhibit superior lubricating properties than other forms of lubrication [28, 29]. Moreover, mixture of solid particles in the base lubricant also exhibited better lubricating properties. The superior role of graphite as a lubricant is validated by the experimentations conducted by various researchers. It is also proved that the size of the solid particles plays a dominant role as a lubricant. The experimental work encompasses the use of graphite as a lubricant in turning operations.

The numerical techniques were used to analyze and interpolate the experimental data obtained during the course of machining for further use. Various techniques and models being used to predict and optimize the machining parameters are fuzzy techniques, regression analysis, neural networks, and Taguchi method [24, 30–33]. Some other models used by researchers were response surface methodology [34, 35] and Taguchi grey relation analysis method of optimization [36–38]. It has been discovered that fuzzy systems can effectively maintain the physical implications and consequences of each variable while simulating highly nonlinear and complex systems [31, 39–42]. Fuzzy systems are widely used for process simulation and control which are designed either from expert knowledge or from experimental data [43, 44].

Recent years have seen the use of numerical methods to evaluate the output machining parameters. One numerical method that assumes a functional dependence between the independent and dependent variables and seeks to minimize modeling error is the regression model. Metal cutting process parameters such as feed force, main cutting force, thrust force, temperature, and surface roughness [45–50] are

predicted using the relations developed. Among the various models to define the relationship between inputs and outputs, power equations [45, 49, 50] are the common ones used to define the relations. It is observed that fuzzy technique is one of the tools which are used to reduce the vagueness of the experimental data. To establish a bond between the input and output parameters, regression modeling is performed. However, it is uncommon to find a model that stresses the impact of lubrication on the machining parameters. Therefore, it is necessary to create a prediction model that includes lubricant as well.

This study encapsulates the use of a range of particle sizes in the nanoregime, which itself is a unique phenomenon, unlike the present-day research findings which used only one particle size for experimentation. The machining input parameters considered for the experimentation has a wide range considered. This study aims at investigating the behavior of nanocrystalline graphite powder as lubricant during the turning of hardened steel under varying machining conditions. This study also includes creating expressions of the experimental results using regression analysis and develops a set of relations which could be used by general users as well as the manufacturers per se.

## 2. Experimental Process

This study aims to investigate the effect of using nanocrystalline graphite powder as lubricant. Turning experiments were conducted using uncoated carbide tools and by varying the input parameters: cutting velocity, feed rate, and depth of cut and using nanocrystalline graphite powder as lubricant. The size of the nanocrystalline graphite powder considered are 5–10, 15–30, 40–60, and 70–90 nm. Initial studies are carried out to find the optimum weight percentage of nanocrystalline graphite powder to be mixed in the carrying medium (SAE 40). It is found that a 0.5 wt% is optimal for the purpose of experimentation. The evaluating parameters of cutting forces, tool tip temperature, and the surface roughness are considered while machining AISI 1040 steel [51, 52] using uncoated carbide inserts. The cutting forces and tool temperatures are measured while the experimentation is being carried out [9] and the surface roughness is found out off-line [53] at the end of each machining process. The cutting forces were measured using a strain gauge lathe tool dynamometer and the tool tip temperature by a K-type thermocouple connected to a temperature calibration unit [54]. Surface roughness of the machined workpiece was measured using surface roughness tester (Tally surf). An indigenously developed liquid particulate dispensing system is attached to the machine for dispersing the lubricant mixture and to take care of agglomeration of the graphite powder mixed in the carrying unit. Experiments are conducted as per full factorial design of experiments [55, 56].

A series of preliminary tests have been carried out to determine the best lubricant flow using the MQL principle. MQL equipment consists of emulsifying equipment and a pipe to dispense the lubricant to the targeted area. Nanoparticulate graphite powder mixed in SAE 40 is applied at the



FIGURE 1: Liquid particulate dispensing unit.

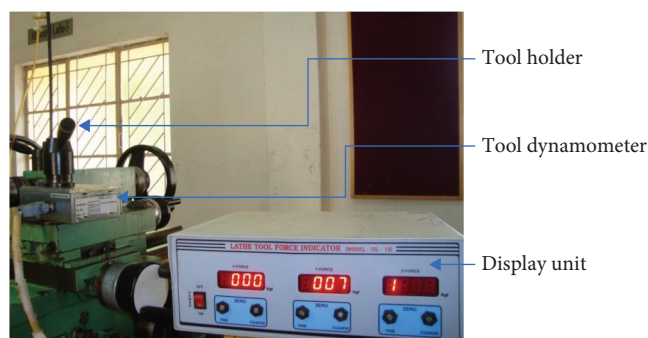


FIGURE 2: Display unit of strain gauge dynamometer.

rate of 10 ml/min. [57]. The experimental setup developed for applying particulate fluid lubricant is shown in Figure 1. Emulsifying equipment is used to maintain the physical composition of the lubricant. The dispensing equipment consists of a reservoir, a stirrer, and a tube used to dispense the lubricant to the targeted area. It helps to keep graphite powder well dispersed in SAE 40 oil during the machining time. After mixing the graphite powder with oil thoroughly in a stirrer, it is poured into the reservoir of the emulsifying equipment. Stirrer is used continuously thus maintaining graphite powder in a well-dispersed form.

In this study, the cutting forces are measured using strain gauge dynamometer which is duly calibrated. The dynamometer is placed in a position as shown in the Figure 2. The tool holder and the display unit of the dynamometer is also shown in the figure.

The thermocouple placed at the bottom of the tool insert measures the temperature. The thermocouple module is shown in Figure 3, and Figure 4 shows the position of thermocouple under the tool tip arrangement.

It is found that the average values of the measured parameters under dry conditions and by using SAE 40 oil are higher than those obtained by the use of nanocrystalline graphite powder as lubricant when considered for all weight percentages and crystalline sizes. Experimental observations revealed that with a 0.5 wt% of nanocrystalline graphite powder mixed in the carrying medium, the cutting forces and the tool tip temperature showed minimum values. The surface quality showed better results than that obtained with other weight percentages. This proves that addition of solid





FIGURE 3: Thermocouple module.



FIGURE 4: Thermocouple arrangement.

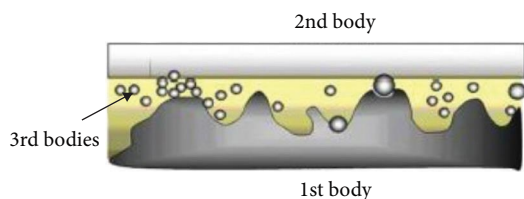


FIGURE 5: Separation of surfaces by a layer of lubricant [58].

particles decreases the cutting forces and the tool temperature and even leads to a better surface finish.

The graphite powder and the carrying medium SAE 40 lubricant mixture demonstrate multifunctional lubrication performance, where surfaces are separated by a liquid lubricant film and protected by solid powder [58].

As depicted in Figure 5, the carrying medium would carry the third-body nanocrystalline graphite powder particles providing lubrication. In preliminary research [58], such a concept was found that there were opposing results in its tribological performance as the size of the solid lubricant was decreased from micron level to nano level. It is due to the fact that more amount of nanoparticles would remain back in the contact zone between the tool and workpiece. The nanoparticles in the contact zone would hold the cutting temperature which would impair the machining

parameters. The phenomenon is explained with the conceptual model developed.

In general, the present experimental results show that the cutting forces, tool temperatures, and surface roughness are found to increase as the size of the nanocrystalline graphite powder is reduced from 70–90 to 5–10 nm, which exhibits an inverse relationship with its size in the nanolevel. This is because more of the smaller graphite particles which remain back in the cutting zone than the larger particles (as depicted in Figure 6). This phenomenon leads to the sticking and interlocking of the solid lubricant particles in the chip–tool interface, thereby increasing the resistance flow of the chip [51]. Tribological test has proved that the powder lubricant would remain back in the contacting region due to the surface tension property of the liquid lubricant [58]. It is also observed in optical microscope images taken on the disk wear tracks after the pin-on-disk tests that more of the smaller particles [51, 58] remained in the wear track than the larger particles.

It is found that a boundary film is formed by the lubricant mixture. As nanocrystalline graphite powder has higher dry coefficient of friction than the SAE 40 oil, there will be increase in the measured parameters when the lubricant loses its viscosity and the nanoparticles remain back in the cutting zone. This mechanism is referred to define the behavior of particles between two surfaces in terms of the size of the particles. But as the temperature raises and at high cutting velocities, the fluid film thickness decreases. This is due to the fact that SAE 40 loses its viscosity at high temperatures. A thin layer of SAE 40 oil between graphite and the cutting surface would be present, but its effect will nullify when the thickness reduces to the nanocrystalline size [59]. Since graphite has a higher dry friction coefficient than SAE 40, it has been deduced that this greater percentage of graphite powder in the sliding contact led to the inverse relationship between particle size and friction coefficient.

The main cutting force is dominated by the depth of cut rather than the other controllable parameters considered for the experimentation. At higher depths of cuts, more amount of material comes in contact with the tool which requires more cutting force to remove the material. The other reason for the increase in the main cutting force is the increase in chip load [60, 61], which increases the energy required to machine the surface. Depth of cut plays a dominant role in the increase of feed force and the thrust force. The increase in the thrust force is due to the fact that at higher depths of cuts, more material is removed thus requiring a higher force. This is also attributed to the fact that with the increase in the depth of cut, the chip thickness becomes significant which causes the growth of volume of the material deformed, and thus enormous cutting force is required to cut the material.

The secondary dominating factor with the increase in the feed force is the cutting velocity. It is observed that there is a substantial effect on the feed force at higher cutting velocities. In general, increase in the cutting velocity leads to a rise in temperature at the cutting zone [53, 62] which makes the metal more plastic, and consequently the efforts necessary for machining decrease. However, due to the increase in

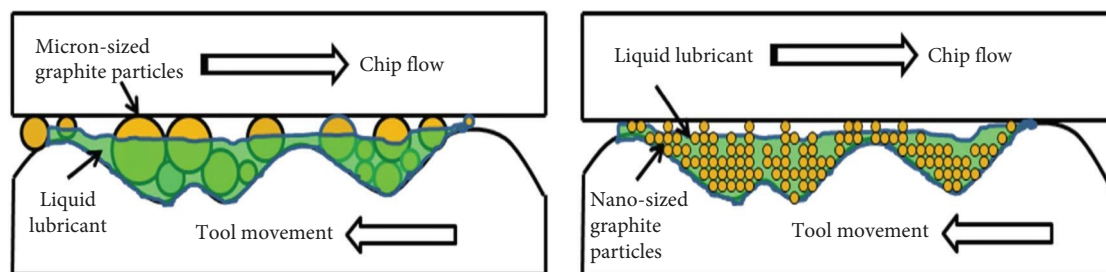


FIGURE 6: Conceptual model depicting the influence of variation particle size in the chip-tool interface.

temperature at the cutting zone, the viscosity of the carrying medium increases which impairs the formation of a layer of fluid film across the cutting surfaces thus increasing the power required to machine the surface [53, 63]. With the increase in the cutting velocity, more amount of material surface comes in contact with the tool as the built-up edges disappear. As the frictional force increases, it is inferred that either the cutting force or thrust force increases or both of the force components increase collectively. At higher cutting velocities, there is a drastic increase in the tool temperatures. The effect of cutting velocity on tool temperature is predominant when compared with other parameters like depth of cut and feed rate. The surface quality deteriorates more with the increase in the feed rate which is a dominating factor when compared with other cutting parameters considered for the experimentation. Surface roughness is a function of feed and for a given nose radius, it changes with the square of the feed rate value. At higher cutting velocities, the surface quality improves due to the fact that the built-up edges disappear with the increase in the cutting velocity [64–66]. This phenomenon is visible in the experimental values obtained during machining, where the surface quality improves with the increase in the cutting velocity.

The graphite powder of lamellar structure which is used for synthesis is procured commercially from Loba Chemme Pvt. Ltd., Mumbai. The crystalline size is found using an X-ray diffractometer which is in the range of 310–347 nm. The commercially procured powder is synthesized into four crystalline sizes to be used in the experimentation. The synthesis of graphite powder is carried out using a high energy planetary ball mill having four jars which rotate simultaneously. The samples were tested periodically by using X-ray diffractometer. In the sample tested after 10 hr of milling using an X-ray diffractometer, the average particle size was found to be 70–90 nm. Further ball milling and subsequent testings at intervals of 10 hr were conducted which ultimately led to the obtainment of the other crystalline-sized graphite powders in the nanoregime.

### 3. Numerical Analysis of the Machining Process

Regression analysis provides a statistical method to establish relationships between a dependent variable and one or more independent variables. Multiple linear regressions are carried out using statistical software called Statistical Package for the Social Sciences (SPSS). It confidently forecasts the results of any experiment or action, assisting in the formulation

of better decisions for a person, division, or organization. In order to reduce modeling error, multiple linear regression assumes a functional dependency between the independent and dependent variables.

The derived relationships were used to forecast several metal-cutting process parameters, including feed force, main cutting force, thrust force, temperature, and surface roughness. Among the various models to define the relationship between inputs and outputs, power equations were developed in this study.

**3.1. Regression Model.** Regression is the process of fitting models for any data. It is the statistical model that is used to predict continuous outcomes based on one or more continuous predictor variables. The average relationship between two or more variables in terms of the original units of the data is measured using regression analysis. There are two categories of variables in regression analysis. The term “dependent variable” refers to a variable whose value is affected or is to be predicted, and the term “independent variable” refers to a variable that influences values or is to be utilized for prediction.

One dependent variable is compared with one independent variable using simple linear regression. Multiple linear regressions are employed when a dependent variable needs to be described in terms of two or more independent variables. Establishing a quantitative relationship between a collection of predictor factors and a response variable is the goal of multiple linear regressions. In order to reduce modeling error, multiple linear regression assumes a functional dependency between the independent and dependent variables. This relationship is useful for understanding which predictors have the greatest effect, and future responses’ values being predicted while just their predictors are currently known.

The beta value is a measure of how strongly each predictor variable influences the response variable (criterion variable) and is measured in units of standard deviation. Thus, the higher the beta value, the greater the impact of the predictor variable on the response variable.

$R$  is a measure of the correlation between the experimental value and the predicted value of the response (criterion) variable.  $R^2$  is called the coefficient of determination and indicates explanatory power of any regression model. Its value lies between “0” and “+1”. It can be shown that  $R^2$  is the correlation between experimental and predicted values. It will reach maximum value when the dependent variable is perfectly predicted by regression.  $R^2$  is the square of this

TABLE 1: Parameter estimates for output variables.

Parameter (feed force)	Estimate (feed force)	Parameter (main cutting force)	Estimate (main cutting force)	Parameter (thrust force)	Estimate (thrust force)	Parameter (temperature)	Estimate (temperature)	Parameter (surface roughness)	Estimate (surface roughness)
$C_1$	39.982	$C_2$	35.277	$C_3$	35.673	$C_4$	13.293	$C_5$	240.054
$\alpha_1$	-0.033	$\alpha_2$	-0.029	$\alpha_3$	-0.033	$\alpha_4$	-0.020	$\alpha_5$	-0.157
$\beta_1$	0.245	$\beta_2$	0.272	$\beta_3$	0.368	$\beta_4$	0.643	$\beta_5$	-0.941
$\gamma_1$	0.146	$\gamma_2$	0.171	$\gamma_3$	0.449	$\gamma_4$	0.734	$\gamma_5$	0.175
$\delta_1$	0.087	$\delta_2$	0.092	$\delta_3$	0.121	$\delta_4$	0.209	$\delta_5$	-0.076

measure of correlation and indicates the proportion of the variance in the response (criterion) variable, which is accounted for by the model. In essence, this is a measure of how good a prediction of the criterion variable can be made by knowing the predictor variables. However,  $R^2$  tends to somewhat overestimate the success of the model when applied to the real world and so an adjusted  $R^2$  value is calculated which takes into account the number of variables in the model and the number of observations (participants) the model is based on. This adjusted  $R^2$  value gives the most useful measure of the success of the model.

**3.2. Nonlinear Expressions for the Output Variables.** It is required to model the process parameters in order to generate appropriate and useful predicted quantitative connections. These models would be quite helpful for adjusting the process parameters. The interpolated results from the fuzzy model are used to model the various responses using the multiple regression approach employing a nonlinear fit between the response and the pertinent significant parameters [48]. Multiple regression analysis was frequently utilized for modeling and interpreting experimental results because it is useful, affordable, and generally simple to use [67–71]. Using analysis of variance (ANOVA), it was possible to determine the importance of the parameters on the outcomes. The mathematical programmer SPSS was used in this work to calculate the regression constants and parameters. In this case, surface roughness prediction models and parameters for the metal-cutting process, such as cutting forces and tool temperatures, were established. The confidence interval taken was 95%. The models were found to be capable of predicting the above parameters with fair accuracy. The regression equations for the output variables are expressed in the preceding equations.

The output parameters expressed in the nonlinear form are represented in the following form:

$$F_x = f_1(S, v, d, f), \quad (1)$$

$$F_y = f_2(S, v, d, f), \quad (2)$$

$$F_z = f_3(S, v, d, f), \quad (3)$$

$$T = f_4(S, v, d, f), \quad (4)$$

$$SR = f_5(S, v, d, f), \quad (5)$$

where  $F_x$  is the feed force,  $F_y$  is the main cutting force,  $F_z$  is the thrust force,  $T$  is the temperature, and  $SR$  is the surface roughness.  $f$  is the response function, and  $S, v, d, f$  represents the input parameters: size of the nanocrystalline graphite powder, cutting velocity, depth of cut, and feed rate, respectively.

The nonlinear form of Equations (1)–(5) which represents the feed force, main cutting force, thrust force, temperature and surface roughness can be written as follows:

$$\text{Feed force: } F_x = C_1(S)^{\alpha_1}(v)^{\beta_1}(d)^{\gamma_1}(f)^{\delta_1}, \quad (6)$$

$$\text{Main cutting force: } F_y = C_2(S)^{\alpha_2}(v)^{\beta_2}(d)^{\gamma_2}(f)^{\delta_2}, \quad (7)$$

$$\text{Thrust force: } F_z = C_3(S)^{\alpha_3}(v)^{\beta_3}(d)^{\gamma_3}(f)^{\delta_3}, \quad (8)$$

$$\text{Temperature: } T = C_4(S)^{\alpha_4}(v)^{\beta_4}(d)^{\gamma_4}(f)^{\delta_4}, \quad (9)$$

$$\text{Surface roughness: } SR = C_5(S)^{\alpha_5}(v)^{\beta_5}(d)^{\gamma_5}(f)^{\delta_5}. \quad (10)$$

The constants  $C_1$  to  $C_5$  and parameters  $\alpha_1$ – $\alpha_5$ ,  $\beta_1$ – $\beta_5$ ,  $\gamma_1$ – $\gamma_5$ , and  $\delta_1$ – $\delta_5$  are then obtained by using nonlinear regression analysis using the interpolated values of the experimental results. The nonlinear solution of the models gives the values of the constants and the parameters which is represented in Table 1.

The equations for the measured parameters in terms of the input parameters are as follows:

$$F_x(\text{feed force}) = 39.982(S)^{-0.033}(v)^{0.245}(d)^{0.146}(f)^{0.087}, \quad (11)$$

$$F_y(\text{main cutting force}) = 35.277(S)^{-0.029}(v)^{0.272}(d)^{0.171}(f)^{0.092}, \quad (12)$$

$$F_z(\text{thrust force}) = 35.673(S)^{-0.033}(v)^{0.368}(d)^{0.449}(f)^{0.121}, \quad (13)$$

$$T(\text{temperature}) = 13.293(S)^{-0.020}(v)^{0.643}(d)^{0.734}(f)^{0.209}, \quad (14)$$

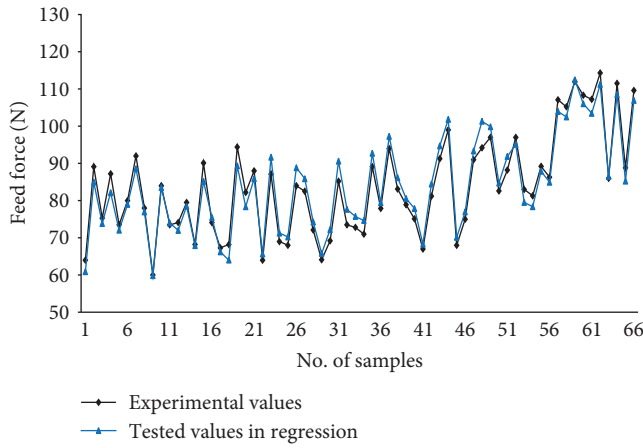


FIGURE 7: Percentage error in feed force.

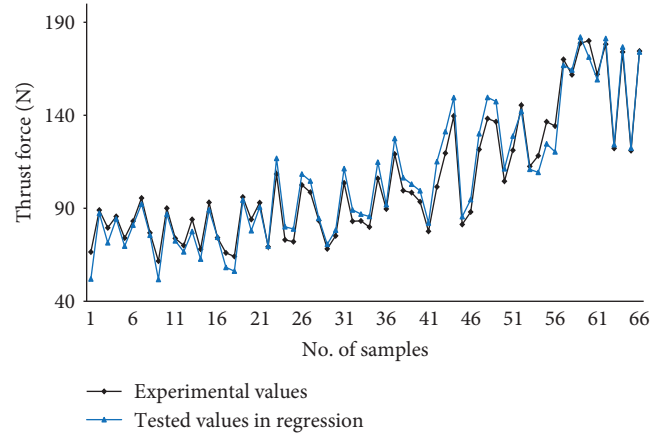


FIGURE 9: Percentage error in thrust force.

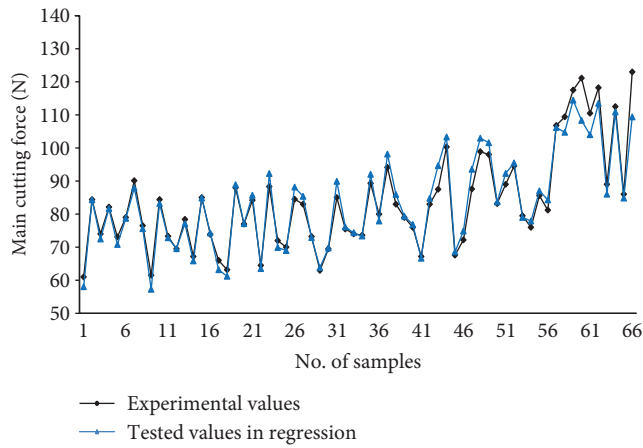


FIGURE 8: Percentage error in main cutting force.

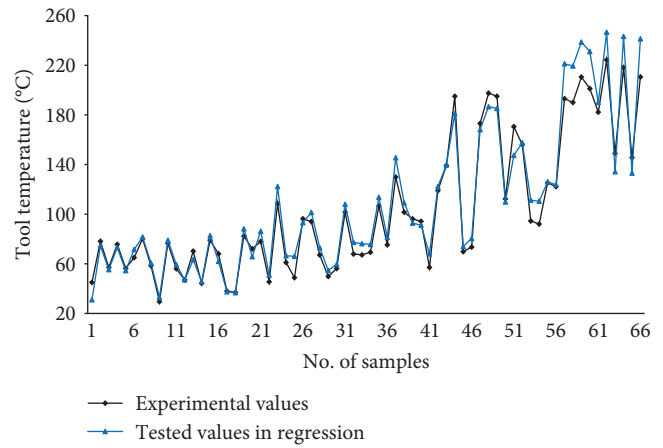


FIGURE 10: Percentage error in tool temperature.

$$SR \text{ (surface roughness)} = 240.054(S)^{-0.157}(v)^{0.941}(d)^{0.175}(f)^{0.076}. \quad (15)$$

#### 4. Validation of the Mathematical Equations

The comparison between the experimental values and the values obtained from the regression equations are depicted in the graphs below. The set of 66 experimental values were used to test the validity of the regression equations developed. The percentage error of the average value of the experimental and tested values for the feed force was found to be 0.23% as shown in Figure 7.

The percentage error of the average values obtained in the main cutting force during experimentation are tested in the equation obtained from regression analysis was 0.23%. It is graphically represented in Figure 8.

The percentage error found between the average values of the experimental and regression equation for thrust force was 0.89%. The difference in the values is depicted in Figure 9.

The percentage error of the average value of the experimental and tested values for the tool temperature was 4.24%. It is represented graphically in Figure 10.

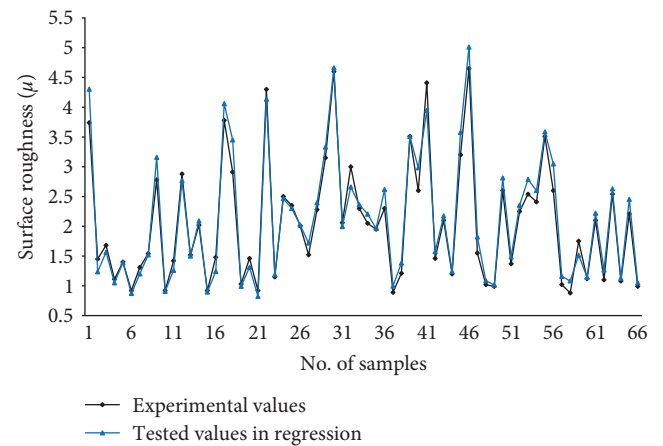


FIGURE 11: Percentage error in surface roughness.

Surface roughness shows an error of 3.46% between the average of the experimental values and was obtained from the regression equation. The values are graphically represented in Figure 11.



TABLE 2: Percentage error between the experimental and predicted values.

Sl. no	Output parameter	Error percentage
1	Feed force	3.92
2	Main cutting force	4.00
3	Thrust force	2.51
4	Temperature	3.09
5	Surface roughness	−1.76

TABLE 3: ANOVA response on feed force (N).

Source	Sum of squares	df	Mean squares
Regression	1,779,803.882	5	355,960.776
Residual	2,193.340	395	8.738
Uncorrected total	1,781,997.223	400	
Corrected total	40,743.784	399	

ANOVA, analysis of variance.

Table 2 represents the error with respect to the tested values and the predicted values using the regression equations developed.

## 5. Results and Discussion

ANOVA was carried out for the output parameter which is explained in the subsequent part.

**5.1. ANOVA Response on Feed Force.** The purpose of this study was to apply a novel method that combines functional data analysis and experiment design. Functional ANOVA was used to measure the effects of several machining parameters on the output parameters, including cutting forces, tool tip temperature, and workpiece surface roughness. All of the information from each test or set of functional data was used in the functional ANOVA. The outcomes of this methodology are described.

From Table 3, a complete realization of the feed force and their effects were achieved. Nonlinear regression analysis was used to model it mathematically.  $R^2$  value was obtained as 0.946 and the adjusted  $R^2$  as 0.9448. It has been noticed that the created model and the experimental findings agree very closely. This implies that the numerical model defined closely confirms the experimental values obtained during machining.

An estimator's mean square calculates the average of the squares of the "errors," or the discrepancy between the estimate and the actual value. According to the expected value of the squared error loss, mean squared error is a risk function [45, 48, 49]. The uncorrected total is the sum of squares of the regression and the residual. The corrected and the uncorrected total relates to the values of regression and the residual sum of squares. Hence, there was no relation between the uncorrected and corrected total with the mean squares [45, 49, 50].

**5.2. ANOVA Response on Main Cutting Force.** As depicted in Table 4, the values required to justify the model are shown.  $R^2$  value was obtained as 0.950 and the adjusted  $R^2$  as 0.9489. It was observed that developed model was in close agreement with the experimental results.

TABLE 4: ANOVA response on main cutting force (N).

Source	Sum of squares	df	Mean squares
Regression	1,760,699.152	5	352,139.830
Residual	2,482.308	395	9.890
Uncorrected total	1,763,181.460	400	
Corrected total	49,307.738	399	

ANOVA, analysis of variance.

TABLE 5: ANOVA response on thrust force (N).

Source	Sum of squares	df	Mean squares
Regression	2,951,224.439	5	590,244.888
Residual	10,453.731	395	41.648
Uncorrected total	2,961,678.170	400	
Corrected total	236,186.724	399	

ANOVA, analysis of variance.

TABLE 6: ANOVA response on temperature ( $^{\circ}\text{C}$ ).

Source	Sum of squares	df	Mean squares
Regression	3,450,135.591	5	690,027.118
Residual	32,103.610	395	127.903
Uncorrected total	3,482,239.201	400	
Corrected total	703,879.449	399	

ANOVA, analysis of variance.

TABLE 7: ANOVA response on surface roughness ( $\mu$ ).

Source	Sum of squares	df	Mean squares
Regression	1,686.910	5	337.382
Residual	13.251	395	0.053
Uncorrected total	1,700.161	400	
Corrected total	342.676	399	

ANOVA, analysis of variance.

**5.3. ANOVA Response on Thrust Force.**  $R^2$  value and adjusted  $R^2$  values found for thrust force were 0.956 and 0.9551, respectively, which show that the model developed to find the thrust force was in close conformity with the experimental values. ANOVA details are shown in Table 5.

**5.4. ANOVA Response on Temperature.** The values required to justify the model are shown in Table 6.  $R^2$  value was obtained as 0.954 and the adjusted  $R^2$  as 0.9531. It was found that the created model and the experimental findings agree very closely.

**5.5. ANOVA Response on Surface Roughness.**  $R^2$  value and adjusted  $R^2$  values found for surface roughness were 0.961 and 0.9602, respectively, which shows that the model developed to find the surface roughness was in close conformity with the experimental values. ANOVA details are shown in Table 7.

## 6. Conclusion

The calculated values of  $R^2$  and adjusted  $R^2$  for all the dependent variables are summarized in Table 8 for the purpose of convenience in dealing with the data.



TABLE 8: Calculated values of  $R^2$  and adjusted  $R^2$ .

Dependent parameter	$R^2$ value obtained	Adjusted $R^2$ value calculated
Feed force	0.946	0.9,448
Main cutting force	0.950	0.9,489
Thrust force	0.956	0.9,551
Temperature	0.954	0.9,531
Surface roughness	0.961	0.9,602

In order to create nonlinear expressions between the input and output variables, regression analysis was done using the statistical tool SPSS. The interpolated data were used to develop the models that predict cutting forces, tool temperatures, and surface roughness using input factors including size of the nanocrystalline graphite powder, depth of cut, feed rate, and cutting velocity for a considerably good range. The tool helps in analyzing and interpreting the data for further use.

This experimental study gives an insight into the effect of nanolevel variation in the crystalline size of graphite powder on the machining of AISI 1040 steel. The major advantage of the present study is the experimentations carried out with varied particle sizes in the nanoregime, which implies that the experimental data gives a robust numerical correlation as obtained in the present study. However, the major disadvantage is the number of experimentations which are to be carried out due to various ranges of the graphite powder. Synthesis of the graphite powder into the nanoregime is a cumbersome process.

## 7. Future Work

Graphite powder due to its chemical structure is more prone to reduce the coefficient of friction between two sliding surfaces. However, as the crystalline size is reduced and varied at the nanolevel, its behavior is completely reversing. Some of the suggestions for future work include using other nanoparticle-sized lubricant powders and verifying these phenomena in other machining processes. Experimental works can be carried out using different workpiece materials, tools, and widening the range of input parameters like feed rate, depths of cuts, etc., and exploring the effects of other process variables and noise. Conformation of the experimental results can be carried out with other analytical tools. More analytical tools can be developed for different cutting tools and materials which can be used for machining processes.

## Nomenclature

$F_x$ : Feed force  
 $F_y$ : Main cutting force  
 $F_z$ : Thrust force  
 $N$ : Force measurement unit “Newton”  
 $T$ : Temperature  
 $^{\circ}\text{C}$ : Temperature measurement unit “Centigrade”  
 $\text{SR}$ : Surface roughness  
 $\mu$ : Roughness measurement unit in “Micron”  
 $f$ : Response function  
 $S$ : Size of the nanocrystalline graphite powder

$v$ : Cutting velocity  
 $d$ : Depth of cut  
 $f$ : Feed rate  
 $C_1$ : Constant in feed force equation  
 $\alpha_1$ : Parameter associated with size of particle in feed force equation  
 $\beta_1$ : Parameter associated with cutting velocity in feed force equation  
 $\gamma_1$ : Parameter associated with depth of cut in feed force equation  
 $\delta_1$ : Parameter associated with feed rate in feed force equation  
 $C_2$ : Constant in main cutting force equation  
 $\alpha_2$ : Parameter associated with size of particle in main cutting force equation  
 $\beta_2$ : Parameter associated with cutting velocity in main cutting force equation  
 $\gamma_2$ : Parameter associated with depth of cut in main cutting force equation  
 $\delta_2$ : Parameter associated with feed rate in main cutting force equation  
 $F_z$ : Constant in thrust force equation  
 $\alpha_3$ : Parameter associated with size of particle in thrust force equation  
 $\beta_3$ : Parameter associated with cutting velocity in thrust force equation  
 $\gamma_3$ : Parameter associated with depth of cut in thrust force equation  
 $\delta_3$ : Parameter associated with feed rate in thrust force equation  
 $C_4$ : Constant in temperature equation  
 $\alpha_4$ : Parameter associated with size of particle in temperature equation  
 $\beta_4$ : Parameter associated with cutting velocity in temperature equation.

## Data Availability

The data used to support the findings of this study are included in the article. Should further data or information be required, these are available from the corresponding author upon request.

## Conflicts of Interest

The authors declare that they have no conflicts of interest.

## Acknowledgments

The authors thank the members of Centre for Nanotechnology, Andhra University College of Engineering, Visakhapatnam, for the help rendered in doing the work.

## References

- [1] S. Shaji and V. Radhakrishnan, “An investigation on surface grinding using graphite as lubricant,” *International Journal of Machine Tools and Manufacture*, vol. 42, no. 6, pp. 733–740, 2002.

- [2] S. Shaji and V. Radhakrishnan, "An investigation on solid lubricant moulded grinding wheels," *International Journal of Machine Tools and Manufacture*, vol. 43, no. 9, pp. 965–972, 2003.
- [3] A. Venu Gopal and P. Venkateswara Rao, "Performance improvement of grinding of SiC using graphite as a solid lubricant," *Materials and Manufacturing Processes*, vol. 19, no. 2, pp. 177–186, 2004.
- [4] S. Shaji and V. Radhakrishnan, "Analysis of process parameters in surface grinding with graphite as lubricant based on the Taguchi method," *Journal of Materials Processing Technology*, vol. 141, no. 1, pp. 51–59, 2003.
- [5] P. N. L. Pavani, R. Pola Rao, and C. L. V. R. S. V. Prasad, "Synthesis and experimental investigation of tribological performance of a blended (palm and mahua) bio-lubricant using the taguchi design of experiment (DOE)," *International Journal of Technology*, vol. 8, no. 3, pp. 418–427, 2017.
- [6] M. Alberts, K. Kalaitzidou, and S. Melkote, "An investigation of graphite nanoplatelets as lubricant in grinding," *International Journal of Machine Tools and Manufacture*, vol. 49, no. 12–13, pp. 966–970, 2009.
- [7] S. Shaji and V. Radhakrishnan, "Application of solid lubricants in grinding: investigations of graphite sandwiched grinding wheels," *Machining Science and Technology*, vol. 7, no. 1, pp. 137–155, 2003.
- [8] D. Jianxin, C. Tongkun, Y. Xuefeng, and L. Jianhua, "Self-lubrication of sintered ceramic tools with  $\text{CaF}_2$  additions in dry cutting," *International Journal of Machine Tools and Manufacture*, vol. 46, no. 9, pp. 957–963, 2006.
- [9] P. Vamsi Krishna and D. Nageswara Rao, "Performance evaluation of solid lubricants in terms of machining parameters in turning," *International Journal of Machine Tools and Manufacture*, vol. 48, no. 10, pp. 1131–1137, 2008.
- [10] A. Das, S. Padhan, S. R. Das, M. S. Alsoufi, A. M. M. Ibrahim, and A. Elsheikh, "Performance assessment and chip morphology evaluation of austenitic stainless steel under sustainable machining conditions," *Metals*, vol. 11, no. 12, Article ID 1931, 2021.
- [11] S. Padhan, S. R. Das, A. Das, M. S. Alsoufi, A. M. M. Ibrahim, and A. Elsheikh, "Machinability investigation of nitronic 60 steel turning using SiAlON ceramic tools under different cooling/lubrication conditions," *Materials*, vol. 15, no. 7, Article ID 2368, 2022.
- [12] H. Bagchi, N. P. Mukherjee, S. K. Basu, and C. G. Tresidder, "Investigation of metal cutting using molybdenum disulphide as a cutting fluid," *Industrial Lubrication and Tribology*, vol. 24, no. 5, pp. 239–258, 1972.
- [13] S. Srikanth, D. V. Padmaja, P. N. L. Pavani, R. Pola Rao, and K. Ramji, "Effect on the performance of the nano-particulate graphite lubricant in the turning of AISI, 1040 steel under variable machining conditions," *International Journal of Mechanical and Mechatronics Engineering*, vol. 12, no. 2, pp. 143–148, 2018.
- [14] S. Srikanth, K. Ramji, B. Satyanarayana, and S. Ramana, "Investigation on turning of AISI 1040 steel with the application of nano-crystalline graphite powder as lubricant," *Proceedings of the Institution of Mechanical Engineers, Part C: Journal of Mechanical Engineering Science*, vol. 228, no. 9, pp. 1570–1580, 2014.
- [15] G. V. S. S. Sharma, C. L. V. R. S. V. Prasad, S. V. Ramana, and P. N. L. Pavani, "Experimental investigations to study the influence of CuO nanoparticle-blended lubricant on surface finish in turning of AISI, 1040 steel and aluminum," *Journal of Machining and Forming Technologies*, vol. 3, no. 4, pp. 73–88, 2016.
- [16] V. Krishna Kanth, D. Sreeramulu, S. Srikanth, M. Pradeep Kumar, K. E. Jagdeesh, and B. Govindh, "Experimental investigation of cutting parameters using nano lubrication on turning AISI, 1040 steel," *Materials Today: Proceedings*, vol. 18, Part 6, pp. 2095–2101, 2019.
- [17] K. C. Sekhar, V. V. Rama Reddy, S. Srikanth, M. Daniel, and S. Kumar, "Investigating the effect of nano crystalline  $\text{MoS}_2$  particles on the surface integrity of turned components," *Materials Today: Proceedings*, vol. 4, no. 8, pp. 7527–7532, 2017.
- [18] S. Srikanth, K. Ramji, and B. Satyanarayana, "Performance profiling of nanoparticulate graphite powder as lubricant in the machining of AISI, 1040 steel under variable machining conditions," *Advanced Materials Research*, vol. 984–985, pp. 15–24, 2014.
- [19] Y.-R. Liu, J.-J. Liu, and Z. Du, "The cutting performance and wear mechanism of ceramic cutting tools with  $\text{MoS}_2$  coating deposited by magnetron sputtering," *Wear*, vol. 231, no. 2, pp. 285–292, 1999.
- [20] N. M. Renevier, H. Oosterling, U. König et al., "Performance and limitations of  $\text{MoS}_2/\text{Ti}$  composite coated inserts," *Surface and Coatings Technology*, vol. 172, no. 1, pp. 13–23, 2003.
- [21] D. Mukhopadhyay, S. Banerjee, and N. S. K. Reddy, "Investigation to study the applicability of solid lubricant in turning AISI, 1040 steel," *ASME Journal of Manufacturing Science and Engineering*, vol. 129, no. 3, pp. 520–526, 2007.
- [22] D. Singh and P. Venkateswara Rao, "Improvement in surface quality with solid lubrication in hard turning," in *Proceedings of the World Congress on Engineering*, pp. 978–988, WCE, July 2008.
- [23] D. Nageswara Rao and P. Vamsi Krishna, "The influence of solid lubricant particle size on machining parameters in turning," *International Journal of Machine Tools and Manufacture*, vol. 48, no. 1, pp. 107–111, 2008.
- [24] L. A. Zadeh, "Fuzzy sets," *Information and Control*, vol. 8, no. 3, pp. 338–353, 1965.
- [25] M. H. Esfe, S. Alidoust, and R. Esmaily, "A comparative study of rheological behavior in hybrid nano-lubricants (HNLs) with the same composition/nanoparticle ratio characteristics and different base oils to select the most suitable lubricant in industrial applications," *Colloids and Surfaces A: Physicochemical and Engineering Aspects*, vol. 643, Article ID 128658, 2022.
- [26] M. H. Esfe, S. Alidoust, S. Esfandeh, D. Toghraie, and E. M. Ardeshiri, "Laboratory and statistical evaluations of rheological behaviour of  $\text{MWCNT-Al}_2\text{O}_3$  (20: 80)/Oil SAE50 as possible modified nano-lubricants," *Colloids and Surfaces A: Physicochemical and Engineering Aspects*, vol. 641, Article ID 128503, 2022.
- [27] N. Suresh Kumar Reddy and P. Venkateswara Rao, "Experimental investigation to study the effect of solid lubricants on cutting forces and surface quality in end milling," *International Journal of Machine Tools and Manufacture*, vol. 46, no. 2, pp. 189–198, 2006.
- [28] A. B. Khoshaim, T. Muthuramalingam, E. B. Moustafa, and A. Elsheikh, "Influences of tool electrodes on machinability of titanium  $\alpha$ - $\beta$  alloy with ISO energy pulse generator in EDM process," *Alexandria Engineering Journal*, vol. 63, pp. 465–474, 2023.
- [29] W. Sami Abushanab, E. B. Moustafa, M. Harish, S. Shanmugan, and A. H. Elsheikh, "Experimental investigation on surface characteristics of Ti6Al4V alloy during

- abrasive water jet machining process,” *Alexandria Engineering Journal*, vol. 61, no. 10, pp. 7529–7539, 2022.
- [30] S. Yaldiz, F. Unsacar, and H. Saglam, “Comparisons of experimental results obtained by designed dynamometer to fuzzy model for predicting cutting forces in turning,” *Materials & Design*, vol. 27, no. 10, pp. 1139–1147, 2006.
- [31] Y. M. Ali and L. C. Zhang, “Surface roughness prediction of ground components using a fuzzy logic approach,” *Journal of Materials Processing Technology*, vol. 89–90, pp. 561–568, 1999.
- [32] S. Guillaume, “Designing fuzzy inference systems from data: an interpretability-oriented review,” *Institute of Electrical and Electronic Engineers Transactions on Fuzzy Systems*, vol. 9, no. 3, pp. 426–443, 2001.
- [33] M. Thangaraj, M. Ahmadein, N. A. Alsaleh, and A. H. Elsheikh, “Optimization of abrasive water jet machining of SiC reinforced aluminum alloy based metal matrix composites using Taguchi-DEAR technique,” *Materials*, vol. 14, no. 21, Article ID 6250, 2021.
- [34] M. Hemmat Esfe and S. Alidoust, “Modeling and precise prediction of thermophysical attributes of water/EG blend-based CNT nanofluids by NSGA-II using ANN and RSM,” *Arabian Journal for Science and Engineering*, vol. 46, pp. 6423–6437, 2021.
- [35] M. Hemmat Esfe, S. Alidoust, E. M. Ardeshiri, and D. Toghraie, “Comparative rheological study on hybrid nanofluids with the same structure of MWCNT (50%)-ZnO (50%)/SAE XWX to select the best performance of nano-lubricants using response surface modeling,” *Colloids and Surfaces A: Physicochemical and Engineering Aspects*, vol. 641, Article ID 128543, 2022.
- [36] G. Alsuruji, T. Muthuramalingam, E. B. Moustafa, and A. Elsheikh, “Investigation and TGRA based optimization of laser beam drilling process during machining of Nickel Inconel 718 alloy,” *Journal of Materials Research and Technology*, vol. 18, pp. 720–730, 2022.
- [37] T. Muthuramalingam, R. Akash, S. Krishnan, N. H. Phan, V. N. Pi, and A. H. Elsheikh, “Surface quality measures analysis and optimization on machining titanium alloy using CO<sub>2</sub> based laser beam drilling process,” *Journal of Manufacturing Processes*, vol. 62, pp. 1–6, 2021.
- [38] I. M. R. Najjar, A. M. Sadoun, M. Abd Elaziz, A. W. Abdallah, A. Fathy, and A. H. Elsheikh, “Predicting kerf quality characteristics in laser cutting of basalt fibers reinforced polymer composites using neural network and chimp optimization,” *Alexandria Engineering Journal*, vol. 61, no. 12, pp. 11005–11018, 2022.
- [39] T. Takagi and M. Sugeno, “Fuzzy identification of systems and its applications to modeling and control,” *IEEE Transactions on Systems, Man and Cybernetics*, vol. SMC-15, no. 1, pp. 116–132, 1985.
- [40] E. Cox, *The Fuzzy Systems Handbook: A Practitioner’s Guide to Building, Using, and Maintaining Fuzzy Systems*, AP Professional, 1994.
- [41] D. G. Schwartz, G. J. Klir, H. W. Lewis, and Y. Ezawa, “Applications of fuzzy sets and approximate reasoning,” *Proceedings of the IEEE*, vol. 82, no. 4, pp. 482–498, 1994.
- [42] E. Daniel Kirby, J. C. Chen, and J. Z. Zhang, “Development of a fuzzy-nets-based in-process surface roughness adaptive control system in turning operations,” *Expert Systems with Applications*, vol. 30, no. 4, pp. 592–604, 2006.
- [43] E. Daniel Kirby and J. C. Chen, “Development of a fuzzy-nets-based surface roughness prediction system in turning operations,” *Computers & Industrial Engineering*, vol. 53, no. 1, pp. 30–42, 2007.
- [44] N. L. P. Puvvada, P. R. Ronanki, and L. P. Chilamkurti, “Experimental investigation to assess the performance and optimization of process parameters of ESM ing process,” *International Journal of Modern Manufacturing Technologies*, vol. 10, no. 2, pp. 58–66, 2018.
- [45] T. Özel and Y. Karpat, “Predictive modeling of surface roughness and tool wear in hard turning using regression and neural networks,” *International Journal of Machine Tools and Manufacture*, vol. 45, no. 4–5, pp. 467–479, 2005.
- [46] W. Bouzid, “Cutting parameter optimization to minimize production time in high speed turning,” *Journal of Materials Processing Technology*, vol. 161, no. 3, pp. 388–395, 2005.
- [47] P. N. L. Pavani, R. Pola Rao, and K. Santa Rao, “Performance assessment and mathematical modeling of process parameters in electrical discharge machining of EN-31 tool steel material using taguchi DOE,” *Engineering Journal*, vol. 21, no. 2, pp. 227–236, 2017.
- [48] A. Venu Gopal and P. Venkateswara Rao, “Selection of optimum conditions for maximum material removal rate with surface finish and damage as constraints in SiC grinding,” *International Journal of Machine Tools and Manufacture*, vol. 43, no. 13, pp. 1327–1336, 2003.
- [49] A. Doniavi, M. Eskandarzade, and M. Tahmasebian, “Empirical modeling of surface roughness in turning process of 1060 steel using factorial design methodology,” *Journal of Applied Sciences*, vol. 7, no. 17, pp. 2509–2513, 2007.
- [50] S. Ranganathan, T. Senthilvelan, and G. Sriram, “Mathematical modeling of process parameters on hard turning of AISI 316 SS by WC insert,” *Journal of Science & Industrial Research*, vol. 68, pp. 592–596, 2009.
- [51] S. V. Ramana, K. Ramji, and B. Satyanarayana, “Influence of nano-level variation of solid lubricant particle size in the machining of AISI 1040 steel,” *International Journal of Materials Engineering Innovation*, vol. 2, no. 1, pp. 16–29, 2011.
- [52] N. R. Dhar, M. W. Islam, S. Islam, and M. A. H. Mithu, “The influence of minimum quantity of lubrication (MQL) on cutting temperature, chip and dimensional accuracy in turning AISI-1040 steel,” *Journal of Materials Processing Technology*, vol. 171, no. 1, pp. 93–99, 2006.
- [53] V. C. Venkatesh and H. Chandrasekharan, *Experimental Methods in Metal Cutting*, Prentice Hall of India Ltd, 1982.
- [54] A. H. Elsheikh, J. Guo, Y. Huang, J. Ji, and K.-M. Lee, “Temperature field sensing of a thin-wall component during machining: numerical and experimental investigations,” *International Journal of Heat and Mass Transfer*, vol. 126, Part B, pp. 935–945, 2018.
- [55] A. Jiju, *Design of Experiments for Engineers and Scientists*, Elsevier Science & Technology Books, 2003.
- [56] D. C. Montgomery, *Design and Analysis of Experiments*, John Wiley and Sons, USA, 2001.
- [57] N. R. Damera and V. K. Pasam, “Performance profiling of boric acid as lubricant in machining,” *Journal of the Brazilian Society of Mechanical Sciences and Engineering*, vol. 30, no. 3, pp. 239–244, 2008.
- [58] M. A. Kabir, C. F. Higgs III, and M. R. Lovell, “A pin-on-disk experimental study on a green particulate-fluid lubricant,” *Journal of Tribology*, vol. 130, no. 4, Article ID 041801, 2008.
- [59] F. Chiñas-Castillo and H. A. Spikes, “Mechanism of action of colloidal solid dispersions,” *Journal of Tribology*, vol. 125, no. 3, pp. 552–557, 2003.

- [60] M. Mosleh, N. D. Atnafu, and J. H. Belk, "Solid lubricant nano particles as wear-reducing additives in sheet metal forming fluids," in *Proceedings of the ASME/STLE 2009 International Joint Tribology Conference*, pp. 9–11, ASME/STLE 2009 International Joint Tribology Conference, Memphis, Tennessee, USA, October 2009.
- [61] S. Kosaraju, V. Anne, and V. Ghanta, "Effect of rake angle and feed rate on cutting forces in an orthogonal turning process," *International Conference on Trends in Mechanical and Industrial Engineering*, vol. May, pp. 150–154, 2011.
- [62] J. A. Eastman, S. R. Phillpot, S. U. S. Choi, and P. Keblinski, "Thermal transport in nanofluids," *Annual Review of Materials Research*, vol. 34, pp. 219–246, 2004.
- [63] A. Daymi, M. Boujelbene, S. Ben Salem, B. Hadj Sassi, and S. Torbaty, "Effect of the cutting speed on the chip morphology and the cutting forces," *Archives of Computational Materials Science and Surface Engineering*, vol. 1, no. 2, pp. 77–83, 2009.
- [64] R. R. Malagi and B. C. Rajesh, "Factors influencing cutting forces in turning and development of software to estimate cutting forces in turning," *International Journal of Engineering and Innovative Technology (IJEIT)*, vol. 2, no. 1, pp. 37–43, 2012.
- [65] C. Cassin and G. Boothroyd, "Lubricating action of cutting fluids," *Journal of Mechanical Engineering Science*, vol. 7, no. 1, pp. 67–81, 1965.
- [66] B. Geoffrey, *Fundamentals of Metal Machining and Machine Tools*, Scripta Book Company, U.S.A, 1983.
- [67] E. J. A. Armarego and R. H. Brown, *The Machining of Metals*, Prentice Hall, New Jersey, 1984.
- [68] P. N. L. Pavani, R. Pola Rao, and S. Srikan, "Performance evaluation and optimization of nano boric acid powder weight percentage mixed with vegetable oil using the Taguchi approach," *Journal of Mechanical Science and Technology*, vol. 29, pp. 4877–4883, 2015.
- [69] L. Reznik, *Fuzzy Controllers*, Oxford, Newnes, 1st edition, 1997.
- [70] M. Mizumoto, "Fuzzy controls under various fuzzy reasoning methods," *Information Sciences*, vol. 45, no. 2, pp. 129–151, 1988.
- [71] P. N. L. Pavani, C. L. V. R. S. V. Prasad, K. Ramji, and S. V. Ramana, "Characterization of wear and prediction of wear zone locations on the rake face using Mamdani fuzzy inference system," *Proceedings of the Institution of Mechanical Engineers, Part B: Journal of Engineering Manufacture*, vol. 232, no. 1, pp. 78–89, 2018.